CrossMark

Anti-epileptogenic and Anti-convulsive Effects of Fingolimod in Experimental Temporal Lobe Epilepsy

Julika Pitsch[1] · Julia C. Kuehn[1] · Vadym Gnatkovsky[2] · Johannes Alexander Müller[1] · Karen M. J. van Loo[1] · Marco de Curtis[2] · Hartmut Vatter[3] · Susanne Schoch[1,4] · Christian E. Elger[4] · Albert J. Becker[1]

Abstract
Temporal lobe epilepsy (TLE) represents a devastating neurological condition, in which approximately 4/5 of patients remain refractory for anti-convulsive drugs. Epilepsy surgery biopsies often reveal the damage pattern of "hippocampal sclerosis" (HS) characterized not only by neuronal loss but also pronounced astrogliosis and inflammatory changes. Since TLE shares distinct pathogenetic aspects with multiple sclerosis (MS), we have here scrutinized therapeutic effects in experimental TLE of the immunmodulator fingolimod, which is established in MS therapy. Fingolimod targets sphingosine-phosphate receptors (S1PRs). mRNAs of fingolimod target S1PRs were augmented in two experimental post status epilepticus (SE) TLE mouse models (suprahippocampal kainate/pilocarpine). SE frequently induces chronic recurrent seizures after an extended latency referred to as *epileptogenesis*. Transient fingolimod treatment of mice during epileptogenesis after suprahippocampal kainate-induced SE revealed substantial reduction of chronic seizure activity despite lacking acute attenuation of SE itself. Intriguingly, fingolimod exerted robust anti-convulsive activity in kainate-induced SE mice treated in the chronic TLE stage and had neuroprotective and anti-gliotic effects and reduced cytotoxic T cell infiltrates. Finally, the expression profile of fingolimod target-S1PRs in human hippocampal biopsy tissue of pharmacoresistant TLE patients undergoing epilepsy surgery for seizure relief suggests repurposing of fingolimod as novel therapeutic perspective in focal epilepsies.

Keywords Disease-modifying therapy · Temporal lobe epilepsy · Epileptogenesis · Experimental epilepsy models · Video-EEG

Introduction

Pharmacoresistance to anti-epileptic drugs occurs in about 30% of epilepsy patients [1, 2]. The most frequent epilepsy

✉ Julika Pitsch
  jpitsch@uni-bonn.de

1   Section for Translational Epilepsy Research, Department of Neuropathology, University of Bonn Medical Center, Sigmund-Freud-Str. 25, 53105 Bonn, Germany

2   Unit of Epileptology and Experimental Neurophysiology, Fondazione Istituto Neurologico Carlo Besta, 20133 Milan, Italy

3   Clinic for Neurosurgery, University of Bonn Medical Center, 53105 Bonn, Germany

4   Clinic for Epileptology, University of Bonn Medical Center, 53105 Bonn, Germany

syndrome with focal seizure onset is temporal lobe epilepsy (TLE), which is pharmacoresistant even in 80% of the patients [3]. In biopsies of chronic pharmacoresistant TLE patients, that underwent epilepsy surgery for seizure control, major neuropathological changes are segmental neuronal cell loss and extensive astrogliosis summarized under the term *hippocampal sclerosis* (HS). Reactive astrocytes and activated microglia are prominent in HS and strongly signal to neurons [4, 5] by release of cytokines including TNF-alpha and IL-1ß as well as also nitric oxide [6]. Anti-epileptic drugs (AEDs) generally act as *anti-convulsants* but do not prevent or reverse the development of drug-resistant epilepsy. "Epileptogenesis" refers to the development of an epileptic condition after a transient brain insult and/or the progression of epilepsy after its establishment [7]. In this context, an "anti-epileptogenic" therapeutic strategy aims at applying a therapy regimen for a limited period after an epileptogenic insult to prevent the emergence of spontaneous recurrent seizures [8]. Improving knowledge on heterogeneous epilepsy pathomechanisms may in this context foster tailored therapies, which can be potentially facilitated by repurposing of potent drugs.

🖄 Springer

Sphingolipids represent a class of biologically active lipids that have key roles particularly in inflammation. They signal through specific G-protein coupled receptors, i.e., sphingosine-1-phosphate receptors (S1PRs) 1–5. Recent data demonstrated S1PRs 1 and 3 to be strongly expressed by astrocytes, which may thereby represent cell targets of the anti-inflammatory effects of fingolimod in multiple sclerosis (MS). However, multiple effects of fingolimod have been claimed, including arresting of lymphocyte egress from secondary lymphoid tissues, reduced neuroinflammation, attenuated microgliosis, increased oligodendrocyte differentiation, and potentially neuroprotection [9].

Here, we have scrutinized the use of fingolimod in experimental TLE. Fingolimod indeed exerted both, robust anti-epileptogenic, disease-modifying and anti-convulsive effects in experimental TLE mouse models. The expression signature of S1PRs in human TLE tissue further suggests the potential to translate this therapy approach into the clinical context.

Material and Methods

Animals

Male C57Bl6/N-mice (Charles River, Sulzfeld, Germany; 55–63 days old, weight 20–24 g) were used for all analyses. All efforts were made to minimize pain and suffering and to reduce the number of animals used, according to the ARRIVE guidelines. Mice were housed under a 12-h light–dark-cycle (light cycle 7 am/7 pm), in a temperature (22 ± 2 °C) and humidity ($55 \pm 10\%$) controlled environment with food/water ad libitum and nesting material (nestlets, Ancare, USA). Animals were allowed at least 1 week of acclimatization to the animal facility before surgery and singly housed after surgery. All procedures were planned and performed in accordance with the guidelines of the University of Bonn Medical Centre Animal-Care-Committee as well as the guidelines approved by the European Directive (2010/63/EU) on the protection of animals used for experimental purposes.

Induction of SE by Suprahippocampal Kainate Acid Application

To induce SE by kainate acid (KA), we applied suprahippocampal (-2AP -1.4ML -1.1DV, [10]) 70 nl KA (20 mM, Tocris) over 2 min directed above the left hippocampal CA1 region [11] using a micropump (WPI) containing a Nanofil syringe (WPI). After injection, the syringe was left for 5 min to avoid any reflux. Control injections were performed with the same volume of 0.9% NaCl. The incidence of inducing SE was 100% without any mortality.

Telemetric EEG/Video Monitoring and Seizure Classification

The electrographic features of fingolimod treated vs. control animals following KA-SE were analyzed with a telemetric EEG/video monitoring system (TL11M2-EET, DSI). Implantation procedure and postoperative treatment were previously described in detail [12–14]. Briefly, narcotized [16 mg/kg xylazine (Xylariem, ecuphar, Belgium) and 100 mg/kg ketamine, i.p. (Ketamin 10%, WDT, Germany)] mice were implanted with depth EEG electrodes directly after KA injection (described above) with subcutaneous transmitter placement on the right abdominal side. Depth electrodes were positioned in hippocampal CA1 (-2AP, 1.4ML, 1,3DV [10]). Correct position of the electrodes was histologically controlled in every animal after the study. Stainless screws in contact with the cerebellar cortex of the simple lobe at the midline (-6AP, 0ML, 0DV) were used to fix the reference electrodes. All implanted mice received analgesic treatment before and once per day for 3 days post operation (5 mg/kg ketoprofen, s.c.; Gabrilen, mibe, Germany).

EEG recording was started continuously (24/7) directly after the operation for 60 days for studying the chronic effect of fingolimod treatment and for 28 days for studying the effect on epileptogenesis. The sampling rate was 1 kHz. Although the minimum life time of the batteries of the transmitter type TL11M2-EET (DSI) is 1.5 month the durability is much longer. To evaluate long-term frequency dynamics, we performed a spectral EEG analysis using fast Fourier transform algorithm (FFT) analyzed in 1 s sliding windows with 0.3 s overlap. To produce final time-frequency representation for the respective recording period, this spectral information was analyzed with the Elpho-EEG software (Gnatkovsky, www.elpho.it) and integrated in 1 h time frames.

We have analyzed this model using an identical analysis paradigm as we have applied before in order to characterize epileptic activity and duration of SE in the pilocarpine SE model [1, 2]. Kainate-induced SE was characterized by an increased EEG activity in all frequency bands similar to pilocarpine-induced SE [12] with significant increase in all power bands. To define severity and duration of kainate-induced SE we analyzed frequency changes in *delta* (0–3.99 Hz), and *gamma* (30–40 Hz) frequency power. Duration of SE was quantified by using a threshold which was calculated by using the mean of the frequency power during 14 days (days 4–18 after SE). SE duration was defined as the time during which band power was above this threshold. SE severity was defined by calculating the cumulative power of each frequency band during SE [12].

Seizures were analyzed within the EEG recordings using the NeuroScore v3.2 (DSI) software with the following parameters: threshold value 100–5000 µV, spike duration 5–70 ms, spike interval 0.005–1 s, minimum train duration of

5 s, and minimum number of spikes per event of 10. The output of all animals was checked manually for false positive events (e.g., artifacts) and all false-positive events were deleted from the output files.

From concurrent video recordings, all spontaneous seizures during the recording time were analyzed using previously described classifications used in the pilocarpine model [15]: seizures were identified by clear epileptiform EEG signals (> 2× baseline peak to peak amplitude) corresponding to an evident behavior in the video: stage III were short seizures with repetitive tonic-clonic forelimb movement and stage VI severe seizures with rearing without falling and stage V severe seizures with rearing and falling/loss of righting ability. Seizures are clearly distinguishable from baseline EEG activity, due to their prolonged (> 12 s) large amplitude signal (for example, see Fig. 5c). Electrographic seizures < 12 s without an evident behavior were not included in this analysis. Information about animal movement activity was obtained from the same implanted transmitters.

SE induced by suprahippocampal KA injection differs from electrophysiological and semiological aspects to SE induced by pilocarpine. Nevertheless, electrophysiological parameters including frequency spectra and cumulative band power increase were similar and were analyzed in the same fashion as for pilocarpine-induced SE. Semiologically, KA-SE differs from SE induced by pilocarpine as KA-SE appears non-convulsive and the behavior turns faster back to normal animal behavior whereas the EEG still showed strong pathology pattern including high-frequency spiking and seizure-like events.

Fingolimod Treatment in Mice

To characterize the potential effect of fingolimod treatment in the context in the context of seizure emergence after SE, we used two separate study designs to separate a disease-modifying, anti-epileptogenic from an anti-convulsive effect. Firstly, we studied the effect of fingolimod treatment in the stage of spontaneous chronic recurrent seizure (study design Fig. 1a; treatment day 47–60, $n = 7$ per group; test of anti-convulsive effect). Secondly, we scrutinized the effect of fingolimod treatment starting 1 h after SE induction for 2 weeks. After this 2-week treatment period, fingolimod administration was discontinued and animals were monitored for another 2 weeks (study design, Fig. 6a; treatment days 1–14, untreated $n = 13$, treated $n = 9$; test of disease-modifying, anti-epileptogenic effect).

For all mice (sham-injected and fingolimod treatment group) the analgetic and narcotic treatment schemes were identical. For the analysis of the treatment during the stage of chronic recurrent seizures only, basal EEG was recorded for 46 days after SE induction. Fingolimod treatment started at day 47 post-SE with a dosage of 2 mg/kg i.p. of fingolimod (Sigma, Germany) for 1 week (days 47–53 after SE) and continued with 6 mg/kg i.p. fingolimod for another week (days 54–60 after SE). The first dosage (2 mg/kg fingolimod) was adapted from rat studies [16, 17]. The second dosage (6 mg/kg) was calculated to be the human equivalent dose (HED) [18]. This calculation converts the dosage from human MS treatment by using the body surface area into animal dosages.

To study the impact of early intervention with fingolimod, mice received a dosage of 6 mg/kg i.p. per day over 2 weeks starting directly 1 h after KA injection. After discontinuing of the fingolimod treatment in weeks 3 and 4, animals were still video-EEG monitored to identify a potential disease-modifying effect (study design, see Fig. 6a). The induction of SE with respect to analgetic and narcotic treatment was completely the same in all animals under study despite of NaCl injection instead of fingolimod (sham-injected and treatment group).

Induction of SE by Systemic Pilocarpine Application

Sustained status epilepticus (SE) was induced by administration of pilocarpine using previously described injection protocols [14, 15]. Briefly, 20 min after subcutaneous injection of a low dose of scopolamine methyl nitrate (1 mg/kg; Sigma, Germany), mice were treated with subcutaneous pilocarpine hydrochloride (335 mg/kg; Sigma, Germany). SE-experienced mice received 40 min after SE onset 4 mg/kg s.c. diazepam (ratiopharm, Germany). Sham-control animals were treated identically, but received saline instead of pilocarpine. After SE, all animals were fed with soaked rodent food and 5% glucose solution. Of pilocarpine-injected animals, only those that developed SE (SE-experienced) were further used for mRNA/protein analyses. This SE model was used for mRNA and protein expression analysis to underline the changes found in the kainic acid-induced SE model.

mRNA Isolation and Real-Time RT-PCR Quantification

mRNA from different microdissected hippocampal regions (DG, CA1, CA3) at different time points after induced SE was isolated using the Dynabeads mRNA Direct™ Micro Kit (Invitrogen) according to the manufacturer's protocol. cDNA was synthesized by reverse transcription using the RevertAid™ Premium First-Strand cDNA Synthesis Kit (Fermentas) following the manufacturer's protocol. S1PR subunit transcript quantification was performed by real-time RT-PCR. Relative quantification of the starting mRNA copy numbers was carried out according to the $\Delta\Delta C_t$ method. The signal threshold was set within the exponential phase of the reaction for determination of the threshold cycle (C_t). PCR samples contained 2× Maxima

SYBR Green qPCR Master Mix (Fermentas), 5 pM each oligonucleotide primer (Suppl. Table 1), and 1.25 μl synthesized cDNA in a 6.25 μl volume. Quantitative PCR was performed in an ABI Prism 7900HT (Applied Biosystems, Foster City, CA, USA) with conditions as follows: 2 min at 50 °C, 10 min at 95 °C, then 40 cycles of 15 s at 95 °C and 1 min at 59 °C.

S1PR3 Protein Expression Analyses After Pilocarpine-Induced SE

For S1PR3 expression studies, mice were decapitated at several time points after SE under deep isoflurane anesthesia (Forene®, Abbott, Germany). Twenty-micrometer-thick slices were cut with a vibratome (microm HM650V, ThermoScientific) stored in 4% PFA. Slices were first washed in 1 ml PBS and blocked for 30 min with Bordey buffer (0.1% Triton X-100, 0.1% Tween 20, 2% BSA in TBS, pH 7.4) at RT. First antibodies (S1PR3, GFAP, Iba-1; for additional information, see Suppl. Table 2) were diluted in the Bordey buffer and incubated over night at 4 °C on a shaking platform. Prior to incubation with respective secondary antibodies, the slices were washed with 1 ml PBS-T (PBS containing 0.3% Triton X-100). The secondary antibodies and DAPI (1:100) were added for 2 h at RT on a shaking platform. Unspecific binding was removed by washing the slices three times for 5 min in 1 ml PBS-T before mounting with Vectashield (vector Laboratories, GB).

Histopathological and Immunohistochemical Analyses After KA-Induced SE

Mice were decapitated under deep isoflurane anesthesia (Forene®, Abbott, Germany), and brains were quickly removed, fixed in 4% PFA overnight, and embedded in paraffin. Neuropathological studies after KA-induced SE of animals with and without fingolimod treatment were done in coronary hippocampal paraffin sections (4 μm) used for both hematoxylin-eosin (H&E) staining and immunohistochemistry. Standard protocols were used for immunofluorescent stainings against the following proteins (for additional information, see Suppl. Table 2): S1PR3, GFAP (glial fibrillary protein; reactive astrogliosis), MAP2 (microtubule-associated protein2; neuronal cytoskeleton), NeuN (neurofilament; neuronal somata), Iba-1 (ionized calcium binding adaptor molecule 1; activated microglia), CD45 (leukocyte common antigene), and CD8 (CD8+ cytotoxic T cells).

Briefly, paraffin sections were de-paraffinized in xylene two times for 10 min followed by decreasing alcohol series (100–50%) for 2 min at each concentration. Slides were then rinsed for 2 min in distilled water. After washing, slides were subjected to a citric acid antigen retrieval procedure, followed by two washing steps in PBS (5 min). Subsequently, brain sections were rinsed for 2 h at 37 °C in PBS blocking buffer [(10% normal goat serum (NGS), 1% fetal calf serum (FCS)] to inhibit non-specific antibody binding. To identify specific brain cells, slides were incubated with primary antibodies over night at room temperature. After washing for two times in PBS slides were incubated with respective secondary antibody and DAPI counterstain 1:100 (Life technologies, Germany) in blocking buffer. After washing, slides were mounted with Mowiol 4-88 (Roth, Germany).

All non-fluorescent digital images were captured with Nikon DS-Vi1 (Nikon, Germany). Fluorescent images were done with a confocal microscope (Nikon, Eclipse Ti). Appropriate placement of the electrodes in CA1 hippocampal area was assessed in all mice in both hemispheres.

Neuronal cell counts within dorsal CA1 and CA3 pyramidal layer was determined in both hemispheres by counting between − 1.6 and − 1.9 mm posterior to Bregma at least 0.3 mm far from electrode placement using a quantification method based on stereological principles. Neurons were evaluated from three sections (200 μm separation distance) per animal with a size > 10 μm in which the entire outline of the cell was apparent at 400× magnification and averaged into single values for each animal by an investigator blinded to the experimental group. Final cell counts were expressed in NeuN-positive neurons per 1000 μm². Analyzed slices had no signs of reactive astrogliosis caused by electrodes within the counted region. NeuN-positive cells were manually counted and marked by using the cell counter plugin and the analyzed area was determined (ImageJ). Final cell counts for CD8+ cells were equivalently counted per 20,000 μm² in both hemispheres. As the samples used here underwent identical methodological procedures, the impact of variability in tissue quality for neuronal cell counts should be minimized and affect in a similar way control and experimental model sections.

GFAP and Iba-1 staining served as qualitative assessment of gliosis as described for human TLE [19]. This staining was rated in severity from 0 to 4 (0 = no reactive gliosis, 4 = strong gliosis) of three independent investigators blinded to the groups [14]. Iba-1 and CD45-staining was quantified in an equivalent manner.

Human TLE Patients and mRNA Expression Analyses

Gene expression analysis was carried out in patients who underwent surgical treatment in the Epilepsy Surgery Program at the University of Bonn Medical Center due to pharmacoresistant TLE. We compared human hippocampal biopsy tissue from patients with hippocampal sclerosis (n = 79) and patients with lesion-associated (low-grade neoplasms or dysplasia; n = 36) chronic TLE. In all patients, pre-surgical evaluation using a combination of non-invasive and invasive procedures revealed that seizures originated in the mesial temporal lobe [20]. All procedures were conducted in accordance

with the Declaration of Helsinki and approved by the Ethics Committee of the University Bonn, Medical Center. Informed written consent was obtained from all patients. Clinical characteristics of the patients were published before [21]. mRNA analysis for S1PR1–5 and β-actin was carried out analogous to a procedure described elsewhere in detail [22]. Briefly, RNA from surgical biopsies (750 ng cRNA) was used for hybridization on Human HT-12 v3 Expression BeadChips with Illumina Direct Hybridization Assay Kit (Illumina, San Diego, CA) according to standard procedures. We extracted data for S1PR1–5 and β-actin analyzed by Illumina's GenomeStudio Gene Expression Module and normalized using the Illumina BeadStudio software suite by quantile normalization with background subtraction.

Statistical Analysis

Statistical analyses were performed with the GraphPad Prism 6.05 software (GraphPad Software). The two-way ANOVA followed by Sidak's post hoc test was used for statistical assessment of phenotypic differences between groups. Group comparisons were carried out using the Mann-Whitney U test. Ordinal data was analyzed using χ^2 test. Values were considered significantly at $p < 0.05$. Results were expressed as mean ± SEM. Ranking results were expressed as median ± interquartile range. All animal experiments were conducted in a randomized and blinded fashion.

Results

Fingolimod Strongly Reduces Seizure Severity and Frequency in Experimental Chronic TLE

Chronic TLE development is recapitulated in mice by induction of SE using systemic or local application of excitotoxic compounds, i.e., kainic acid or pilocarpine. To analyze the impact of fingolimod treatment in an established post-SE TLE mouse model, we induced SE by unilateral injection of kainate (KA) in a suprahippocampal localization above the left CA1 region [11]. This model reliably induces chronic seizures originating from the hippocampus and reflects key histopathological HS changes including segmental neuronal cell loss and reactive astrogliosis but lacks the immediate cytotoxic effects on hippocampal neurons that are present when injecting kainic acid into the hippocampal formation immediately and avoids traumatic CA1 damage [11, 23]. We continuously (24/7) recorded video-EEG for an extended time span of 2 months ($n = 7$ per group). Fingolimod was administered transiently only in the chronic recurrent seizure period (days 47–60 after SE). All mice developed spontaneous chronic seizures in an identical fashion before they were randomly separated into fingolimod-treated versus control groups.

Seizure frequency and severity were quantified in all animals (study design, Fig. 1a). Seizure frequency was strongly decreased in fingolimod-treated animals (orange bars) compared to non-treated mice (gray bars) after SE-induced TLE (Fig. 1b) when treated with a dosage of 2 mg/kg (days 47–53; Fig. 1b, leftmost) or 6 mg/kg (days 54–60; Fig. 1b, rightmost). Furthermore, comparing seizure frequency of the same animals before (days 5–47; Fig. 1d, e, red bars) and after (days 54–60; Fig. 1d, e, black bars), the onset of pharmacotreatment revealed a substantial reduction under 6 mg/kg fingolimod application (Fig. 1d) as well as less severe seizures (Fig. 1e) in respective mice. No side effects such as weight loss or other behavioral changes were noticed under chronic fingolimod treatment and all mice in the study survived.

Representative cumulative power of different frequency bands (0–50 Hz) is represented in 1-h bins of one treated SE animal (Fig. 1c). Sequences of light and dark vertical columns indicate the cycles of circadian 24 h EEG power density. SE is characterized by an increase of beta-gamma activity (days 0–2) seen as a lightning at the beginning of the spectrogram (Fig. 1c), which was absent in the sham-injected non-SE animal. Seizure frequency of the representative SE animal is shown in blue bars above the spectrogram with a latency of 10 days and a slight increase of seizure frequency over time, which is evidenced by an increase in all analyzed frequencies and characterized by a lightning in the spectrogram (days 40 to 49). This increased lightening in the spectrogram was absent in all analyzed sham-injected fingolimod-treated control animals. Under fingolimod treatment, the EEG shows a strong decrease in all frequency bands reflected by a darkening in the color scheme of the spectrogram illustrating a deactivation starting around day 49 after SE.

We next correlated the spectrogram changes with the movement/activity of the respective animal (Fig. 1c, lower traces). Movement activity of the SE mice showed a transient increase during/after SE induction (days 1–7), followed by a decrease for several days (days 8–18 after SE), afterwards resulting in a relatively stable correlation between circadian changes and movement/activity in the later chronic phase (from day 19 after SE) characterized by the occurrence of spontaneous chronic recurrent seizures. In the sham-injected non-SE animal, the activity appeared more stable over the entire recording time.

Distinct mRNA Augmentation of S1PR Subunits in Experimental Chronic TLE

To identify the underlying mechanisms of this strong antiepileptic effect in vivo, we studied the mRNA expression of the fingolimod target molecules S1PRs1, 3, 4, and 5 in brain tissue samples after pilocarpine- and KA-induced SE. In naïve control CA1, we found the expression levels of S1PR2 and 4 mRNA to be of very low abundance (Suppl. Fig. 1A). We
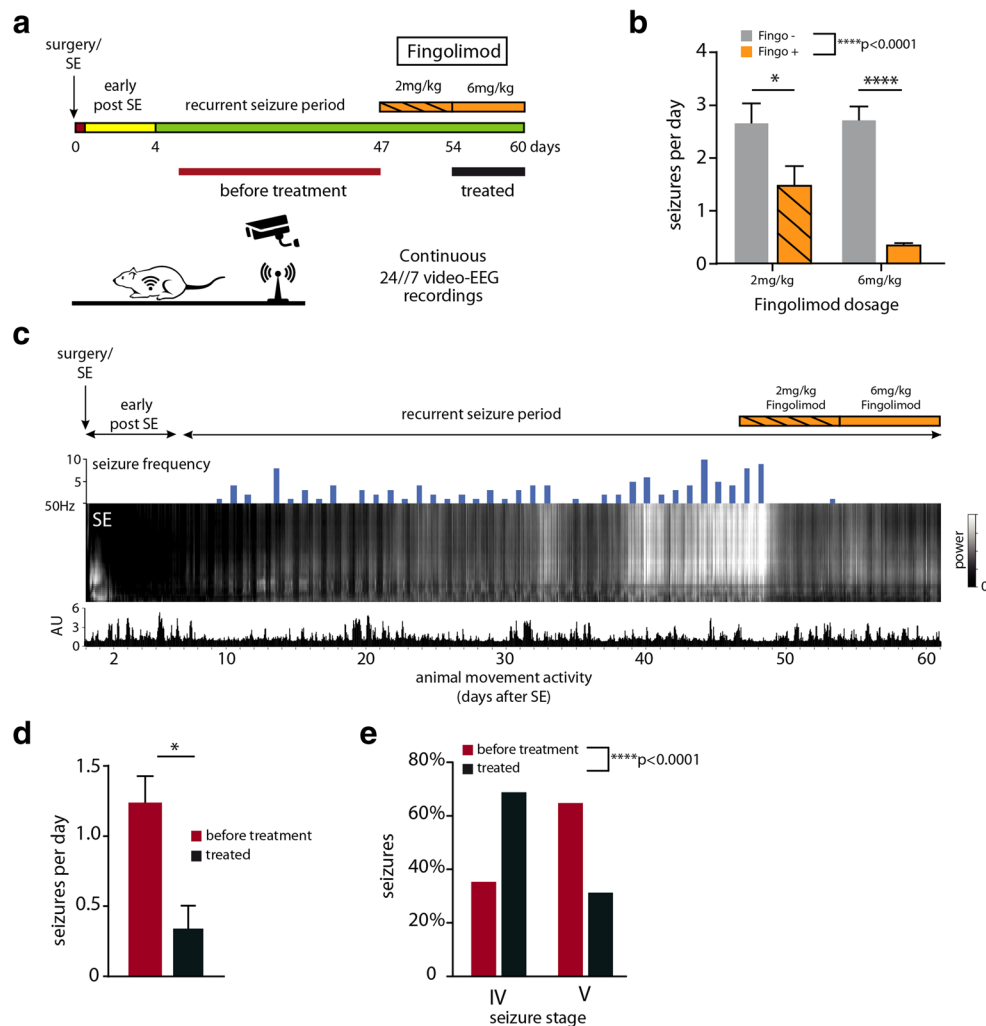
Fig. 1 Fingolimod strongly reduces seizures in chronic epilepsy. **a** Experimental protocol for studying anti-convulsive effects of fingolimod in kainate-induced TLE in the phase of spontaneous chronic recurrent seizures. Day 0: SE induction and electrode implantation. Fingolimod treatment starts at day 47 after SE (days 47–53) with 2 mg/kg fingolimod for 1 week and is continued with 6 mg/kg fingolimod for another week (days 54 to 60). **b** Fingolimod treatment strongly reduces seizure frequency in chronic TLE comparing fingolimod-treated and sham-treated animals at days 47–60 after SE ($n = 7$ per group). Two-way ANOVA: group: ****$p < 0.0001$, $F(1/24) = 35.13$; Sidak's post hoc: 2 mg/kg fingolimod treatment *$p = 0.02$, 6 mg/kg fingolimod treatment ****$p < 0.0001$. **c** Representative power frequency analysis of continuous EEG recording of 60 days (24/7) of a treated SE animal. Time-frequency spectrogram shows normalized cumulative power in "1-h bins." Sequences of light and dark vertical columns indicate the cycles of circadian 24 h EEG power density. Movement activity counts (AU) of the same animal is illustrated in the row under the spectrogram. SE is induced at the beginning of the spectrogram and visible in the activated frequencies mainly between 0 and 30 Hz, which was absent in sham-injected non-SE animals. Seizure frequency of the respective animal is presented in blue bars above the spectrogram. Increase of seizure frequency is strongly correlated with an increase in activity in all analyzed frequency bands visualized in a robust brightening. Low-dose as well as high-dose treatment of fingolimod results in permanent power decrease in the spectrogram (days 49–60 after SE). **d** The frequency of spontaneous recurrent seizures is significantly reduced by 6 mg/kg fingolimod treatment compared to the period before treatment in the same animals ($n = 7$; Mann-Whitney test *$p = 0.0121$). **e** Under fingolimod treatment in the phase of spontaneous chronic recurrent seizures, seizure severity is significantly reduced ($n = 7$; chi-square test ****$p < 0.0001$). Error bars indicate mean ± SEM

further concentrated on the expression levels of the receptor subtypes S1PR1 and 3 after SE, since S1PR2 is not targeted by fingolimod [24] and S1PR4 as well as S1PR5 did not reveal any relevant significant changes in mRNA expression after pilocarpine SE induction (Suppl. Fig. 1B, C).

Real-time quantification was performed starting from different microdissected hippocampal regions (CA1, CA3, and dentate gyrus (DG)) in the stage of chronic recurrent epileptic seizures (28 days after SE induction by KA or pilocarpine). In order to verify that the expression changes have a general impact in epileptogenesis/epilepsy, we analyzed the expression pattern in these two post-SE models (KA and pilocarpine). S1PR1 showed a very prominent mRNA augmentation in CA3 after induction of SE by KA (Fig. 2a) as well as in
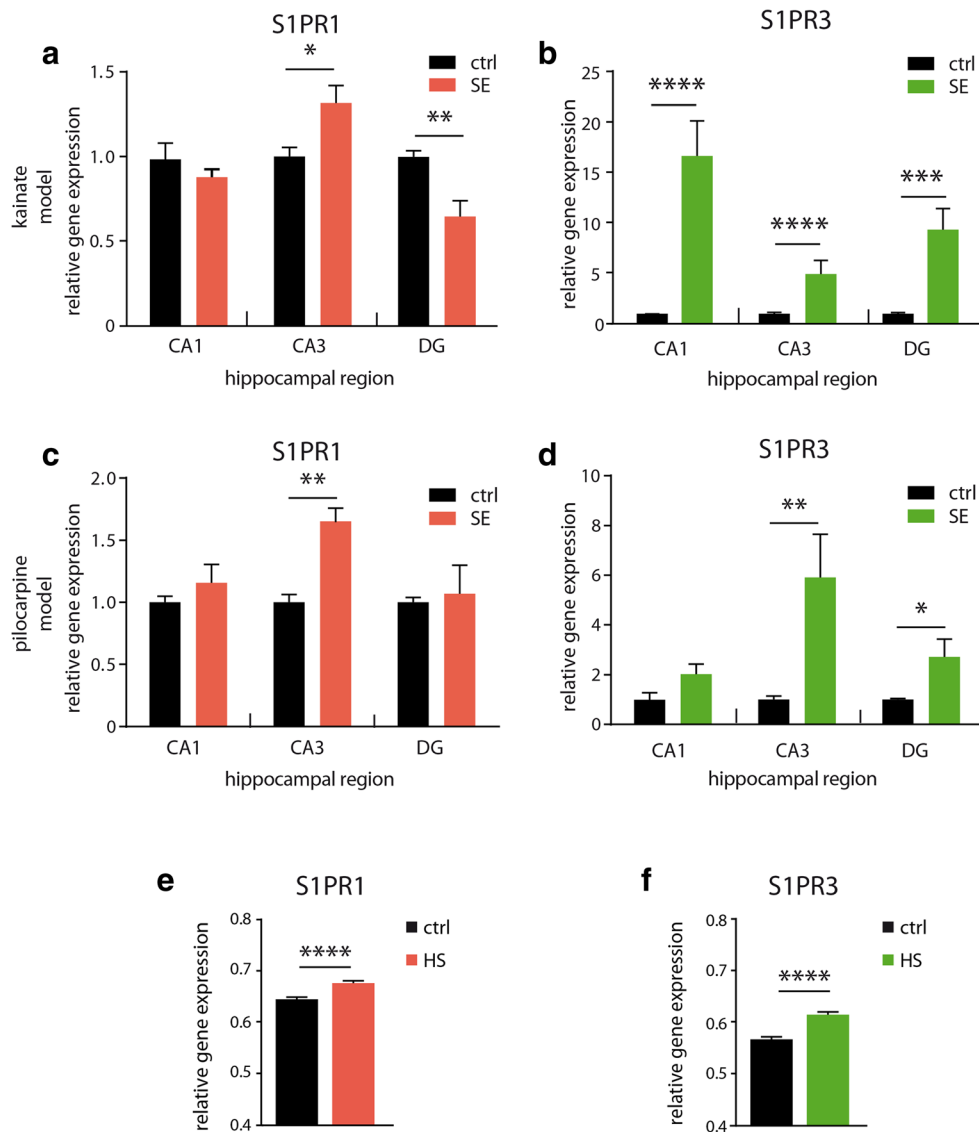
Fig. 2 Hippocampal mRNA abundance of specific S1PRs in experimental and human chronic TLE. Quantitative determination of S1PR1 and S1PR3 mRNA of mice after kainate-induced (**a**, **b**) and pilocarpine-induced (**c**, **d**) SE in different hippocampal subfields compared to sham-injected controls normalized to β-actin. S1PR1 mRNA level is increased in the stage of chronic recurrent seizures **a** after kainate-induced SE in CA3 ($n \geq 10$; Mann-Whitney test $*p = 0.016$) and decreased in DG (Mann-Whitney test: DG $**p = 0.0059$) whereas CA1 is unaffected. **b** S1PR3 is significantly increase in all hippocampal subfields ($n \geq 10$; Mann-Whitney test: CA1, CA3 $****p < 0.0001$, DG $***p = 0.0005$). After pilocarpine-induced SE, S1PR1 (**c**) mRNA is augmented in hippocampal CA3 region ($n \geq 5$; Mann-Whitney test $*p = 0.0022$) and not affected in CA1 and DG whereas **d** S1PR3 is abundant in CA3 ($n \geq 5$; Mann-Whitney test $**p = 0.0043$) and DG (Mann-Whitney test $*p = 0.016$) and not significantly changed in CA1. **e**, **f** Quantitative determination of S1PR1 and S1PR3 mRNA in human TLE. **e** S1PR1 (HS: $n = 79$; control: $n = 36$; Mann-Whitney test $****p < 0.0001$) as well as **f** S1PR3 are significantly more abundantly expressed in hippocampal tissue of TLE patients with HS versus hippocampi from control patients with lesion-associated TLE, in which seizures are explained by lesions such as low-grade neoplasms and/or focal dysplasia in the immediate vicinity or even including the hippocampal formation (HS: $n = 79$; control: $n = 36$; Mann-Whitney test $****p = 0.0001$, with β-actin as reference gene). Error bars indicate mean ± SEM

CA3 in the pilocarpine model (Fig. 2c), whereas it was significantly downregulated in DG after KA-SE (Fig. 2a). S1PR3 was significantly increased after KA-induced SE in all analyzed hippocampal regions (Fig. 2b). After pilocarpine-induced SE, the augmented expression was recapitulated for the CA3 and DG subfields (Fig. 2d). These data suggest a high abundance of S1PR mRNA in hippocampi of both post-SE

TLE mouse models, putatively reflecting susceptibility for fingolimod.

Interestingly, the increased expression levels of S1PR1 and 3 mRNAs in CA3 are correlated to the severity of HS-related neuropathological alterations. Mice, which developed moderate granule cell dispersion in the dentate gyrus and a slight neuronal cell loss representing a mild type of HS do not

exhibit an augmented expression of S1PR1 and 3. In contrast, animals with a strong phenotype depicted in complete granule cell dispersion as well as a severe neuronal cell loss within the hippocampus show a strong expression of S1PR1 (Suppl. Fig. 2A) and 3 mRNAs (Suppl. Fig. 2B).

Increased S1PR1 and S1PR3 Expression Correlate in Human HS

To assess the potential role of S1PRs in human TLE, we analyzed hippocampal S1PR1 and S1PR3 expression levels in pharmacoresistant TLE patients with HS compared to patients with "lesion-associated" TLE (dysplasia, low-grade tumors). The latter are generally regarded as "epileptic controls" for the HS pathology pattern in TLE, since "lesion-associated" patients generally lack initial brain insults inducing epileptogenesis. Interestingly, also in human hippocampal tissue of patients with pharmacoresistant chronic TLE and HS compared to "lesion-associated" cases, we observed a highly abundant expression of S1PR1 and S1PR3 mRNA using β-actin as a reference gene (Fig. 2e, f), which strongly reflects the expression signature of the TLE mouse models described above.

Fingolimod Treatment Substantially Attenuates Reactive Astrogliosis, Neuronal Loss, and Immune Cell Infiltrates After SE

To assess the impact of fingolimod treatment in the stage of chronic recurrent seizures on cellular and structural dynamics in hippocampi after SE induction by excitotoxic compounds, we carried out neuropathological analyses of brains in the stage of chronic epilepsy and compared fingolimod-treated ($n = 8$) with sham-treated mice ($n = 8$) developing chronic TLE after KA-induced SE (study design, Fig. 1a).

Fingolimod-treated animals exhibited significantly less severe neuronal cell loss in CA3 in the injected left hippocampus (representative staining to be found in Fig. 3a, b, left panels; Fig. 3d) but not in CA1 (Fig. 3c), whereas the contralateral site was unaffected by fingolimod treatment. These findings may suggest neuronal degeneration to occur still in the later, chronic stage of the model. Interestingly, reactive astrogliosis was also less severe in animals treated with fingolimod in the ipsilateral as well as in the contralateral hippocampus (representative staining in Fig. 4a, d; Fig. 4c, d). Additionally, a certain variability in the cellular density was observed, even though no quantitatively significant changes regarding the presence and distribution of activated microglia were present (ipsilateral: median ± interquartile range: untreated 1.83 ± 1, treated 1.83 ± 0.71, Mann-Whitney test $p = 0.92$; contralateral: untreated 1.33 ± 1.75, treated 1.83 ± 1.75, Mann-Whitney test $p = 0.85$; representative Iba-1 staining Fig. 3a, b, lower panels). We next analyzed the presence of CD45-positive elements. These analyses revealed reduced CD45-infiltrates in both, ipsi- and contralateral hippocampi of mice after SE, when they received fingolimod (representative immunohistochemistry Fig. 5a). The quantification of CD45-positive cells revealed a decrease in immunoreactivity in the fingolimod treated animals (ipsilateral: Fingo− mean 3 ± 0.7 SD, Fingo+ mean 1.88 ± 0.84, Mann-Whitney test *$p = 0.032$; contralateral: Fingo− mean 2.38 ± 0.74 SD, Fingo+ mean 1.5 ± 0.93, Mann-Whitney test *$p = 0.046$). The incidence of cytotoxic T cells was verified with a CD8-positive immunohistochemistry showing also a reduced amount of CD8-positive T lymphocytes in fingolimod-treated animals (representative immunohistochemistry Fig. 5b, quantification Fig. 5c).

When we compared the KA-injected versus the contralateral hemisphere with respect to reactive astrogliosis (Fig. 4c, d) and neuronal damage (Fig. 3c, d), both aspects were significantly more pronounced within the KA-injected (left) hippocampus than in the contralateral (right) hippocampus. Concerning microglia activation, no significant differences were found between both hemispheres (ipsilateral: Mann-Whitney test $p = 0.15$; contralateral: Mann-Whitney test $p = 0.4$; representative Iba-1 staining Fig. 3a, b).

Overall, the histopathological analyses indicate that fingolimod treatment robustly attenuates segmental neuronal cell loss, reactive astrogliosis, and immune cell infiltrates when the drug is administered in mice during the stage of late chronic epileptic seizures.

Fingolimod Exerts Disease-Modifying Effects in Mice Subjected to SE

We next aimed to test the effect of fingolimod on epileptogenic cascades by treating animals early after SE onset. The experimental dissection of SE-modifying versus anti-epileptogenic effects of pharmacological compounds represents a matter of ongoing debates. However, starting drug treatment only after SE is terminated represents a very artificial regimen in any clinical setting (untreated $n = 13$, fingolimod treated $n = 9$). Here, our aim was to reflect the expectable clinical drug treatment scenario in a most realistic fashion in the present preclinical context. Therefore, respective animals were left in SE for 1 h before we started treatment with fingolimod in a subset of animals for 2 weeks and were compared to sham-injected SE animals (study design, see Fig. 6a). The SE induction protocol including analgesic and anesthetic treatment was completely identical in both groups (sham injected and fingolimod treated). As may be expected, the initial acute phase of SE was neither in electroencephalographical nor in semiological terms different between the individual groups of animals under study (*gamma*; Suppl. Fig. 3A–D). Intriguingly, the following termination phase of the SE was associated with synchronous slow-wave high-amplitude activity which was extended in

Fig. 3 Chronic fingolimod treatment exerts neuroprotective effects. Representative immunohistochemistry of ipsilateral (**a**) and contralateral (**b**) hippocampi of untreated (leftmost panel) and fingolimod-treated mice (middle panel) compared to treated non-SE control mice (rightmost panel, $n = 8$ for all groups). **a** NeuN immunohisto-chemistry reveals the robust granule cell dispersion developing after SE in ipsilateral dentate gyrus, **b** which is absent in the contralateral side whereas the level of activated microglia is un-affected (lower panels). Quantification of neuronal cell loss of CA1 (**c**) and CA3 (**d**) demonstrates a neuroprotective effect of fingolimod in the ipsi-lateral CA3 area ($n = 8$ for each group; two-way ANOVA ***$p = 0.0006$, $F(1,28) = 14.84$. Sidak's post hoc: ipsilateral ****$p < 0.0001$) but not in CA1 ($p = 0.1044$; $F(1,28) = 2.817$). Error bars indicate mean ± SEM
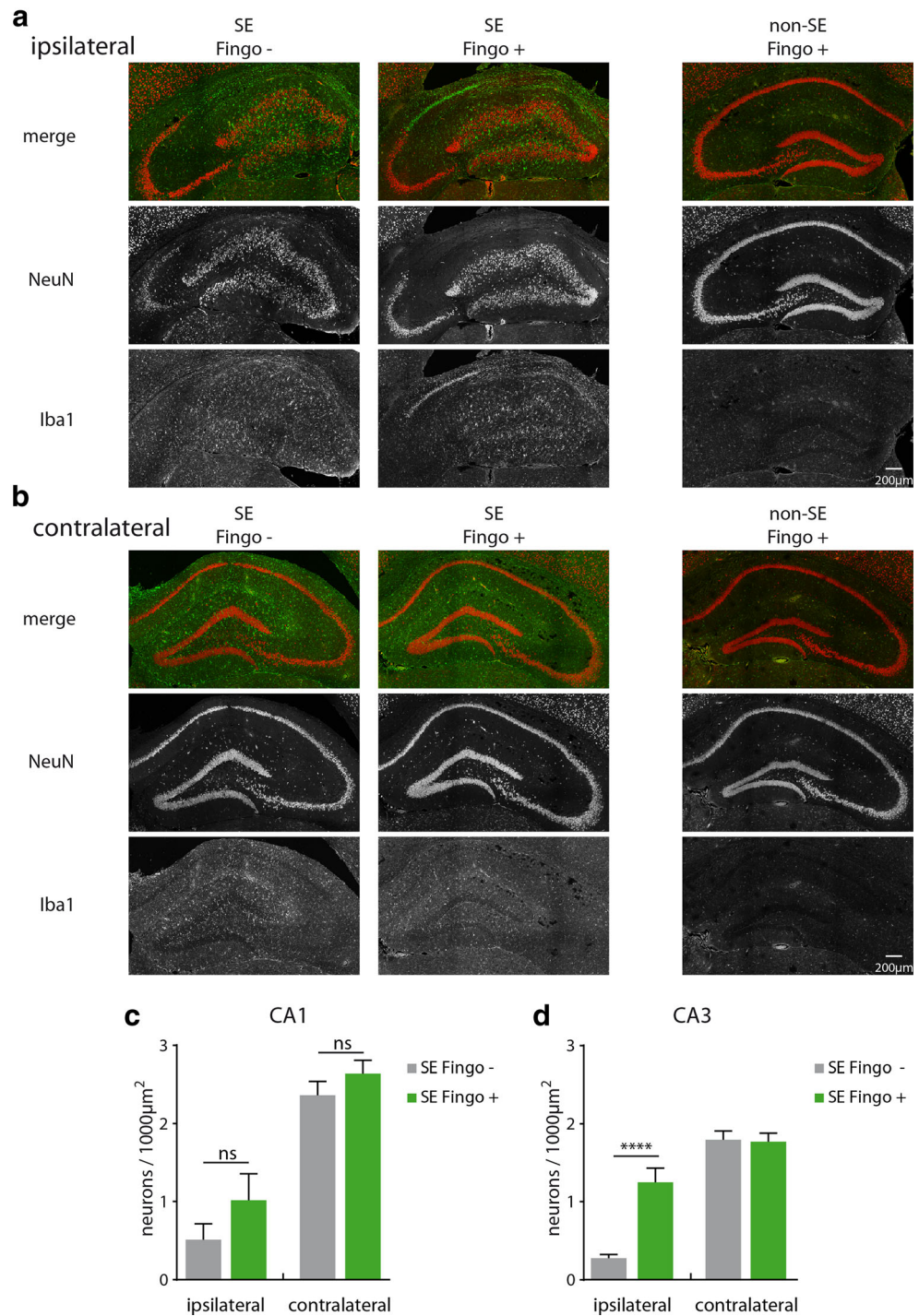
treated animals. This period of SE revealed pathological changes of the EEG but did not have corresponding abnor-malities in the animal behavior. The associated *delta* EEG spectral pattern increase and duration was significantly in-creased in fingolimod-treated animals (*delta*; Suppl. Fig. 3A–D). This terminal phase of SE was not correlated with any seizure like behavior and the animal behaved normally.

In the present animal model, seizures appeared at an early time point after SE induction (2.9 ± 0.47 SEM days). The fingolimod-treated group did not show significant changes with respect to the seizure free interval (4.5 ± 1.4; Mann-Whitney U test $p = 0.29$). A significant reduction of the sei-zure frequency commenced immediately in the first 2 weeks after SE (untreated $n = 13$, fingolimod-treated $n = 9$; Fig. 6b). Even after discontinuing the fingolimod administration in weeks 3 and 4, animals exhibited significant fewer

Fig. 4 Attenuated reactive astrogliosis after fingolimod treatment in chronic TLE. **a**, **b** Representative hippocampal immunohistochemistry of the injected ipsilateral and contralateral side with antibodies targeting GFAP as well as MAP2 of untreated and treated SE animals and treated non-SE animals as control. The ipsilateral (**c**) as well as the contralateral hippocampi (**d**) of treated mice ($n = 7$) show a reduced reactive astrogliosis compared to untreated animals ($n = 8$). The staining was rated in relative extent of astrogliosis from 0 to 4 (0 = no reactive gliosis, 4 = strong gliosis). Mann-Whitney test: ipsilateral *$p = 0.026$, contralateral *$p = 0.024$. Error bars indicate median ± interquartile range
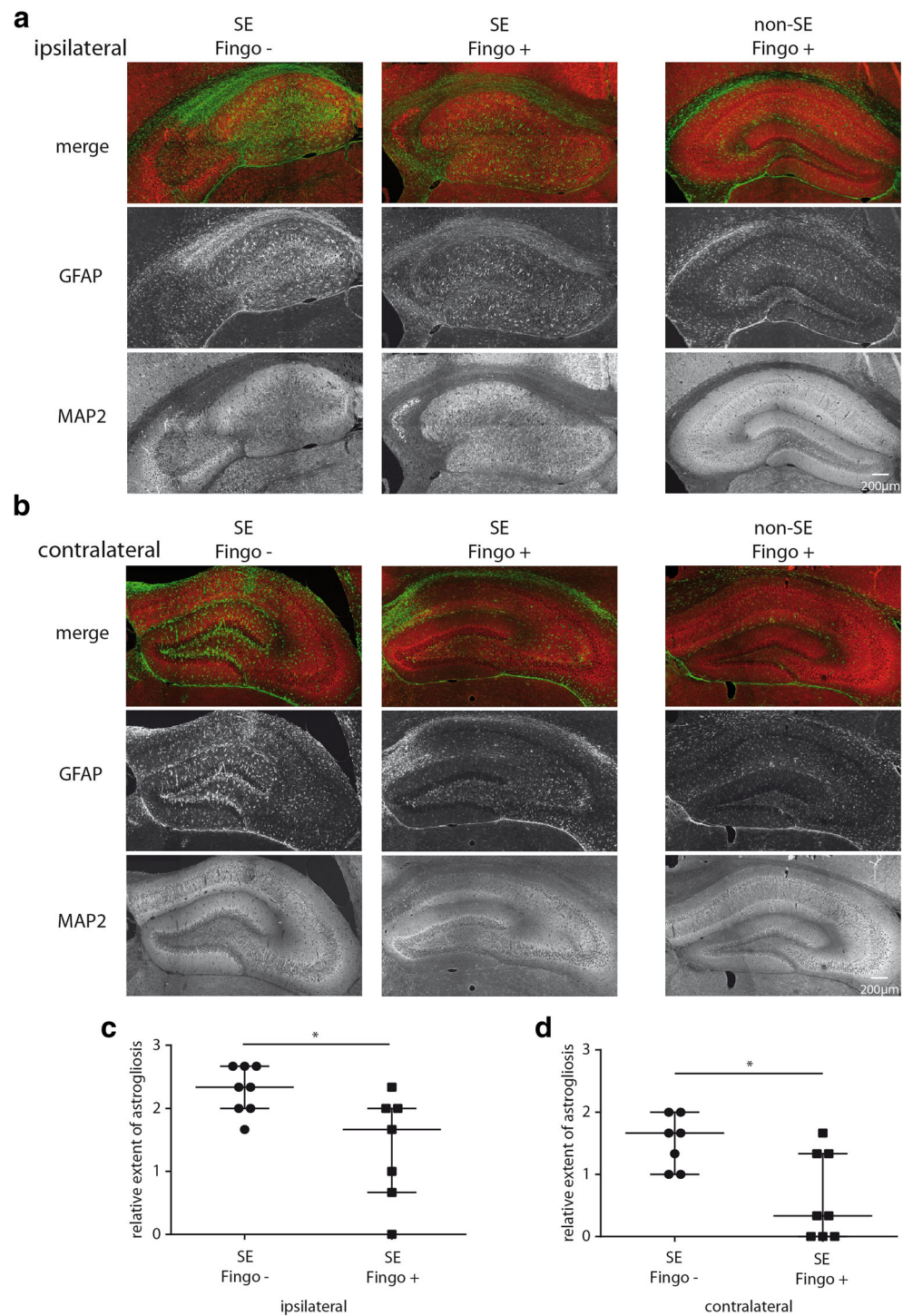
seizures (Fig. 6b). Fingolimod-treated mice exhibited significantly shorter stage V seizures compared to sham-injected control animals (representative seizures of an untreated (Fig. 6c) and fingolimod-treated mouse (Fig. 6d)). This was present during early treatment (weeks 1 and 2, Fig. 6e) as well as after discontinuing fingolimod treatment in weeks 3 and 4 (Fig. 6f). Fingolimod had no effect on seizure

severity. Under fingolimod treatment during weeks 1 and 2 after SE induction seizure severity was unaffected (chi-square test $p = 0.64$). Additionally, in weeks 3 and 4 after SE when fingolimod treatment was stopped, no differences were found between the treated or untreated group with respect to seizure severity (chi-square test $p = 0.86$). Mice did not exhibit any remarkable side effects, weight loss, or

Fig. 5 Reduced cytotoxic T cell infiltrates after fingolimod treatment in chronic TLE. **a** Representative immunohistochemistry of hippocampi of the injected ipsilateral side with antibodies against CD45 (red) and GFAP (green) of untreated and fingolimod-treated SE animals as well as fingolimod-treated non-SE animals as control. DAPI was used as a counterstain. **b** Representative staining of CD8+ cytotoxic T cells (red) confirmed the finding and shows a reduction in the treated group. The ipsilateral (**c**) as well as the contralateral hippocampi (**d**) of treated mice ($n = 8$) show a reduced presence of CD8$^+$ cells compared to untreated animals ($n = 8$). Mann-Whitney test: ipsilateral ***$p = 0.00022$, contralateral ***$p = 0.0009$
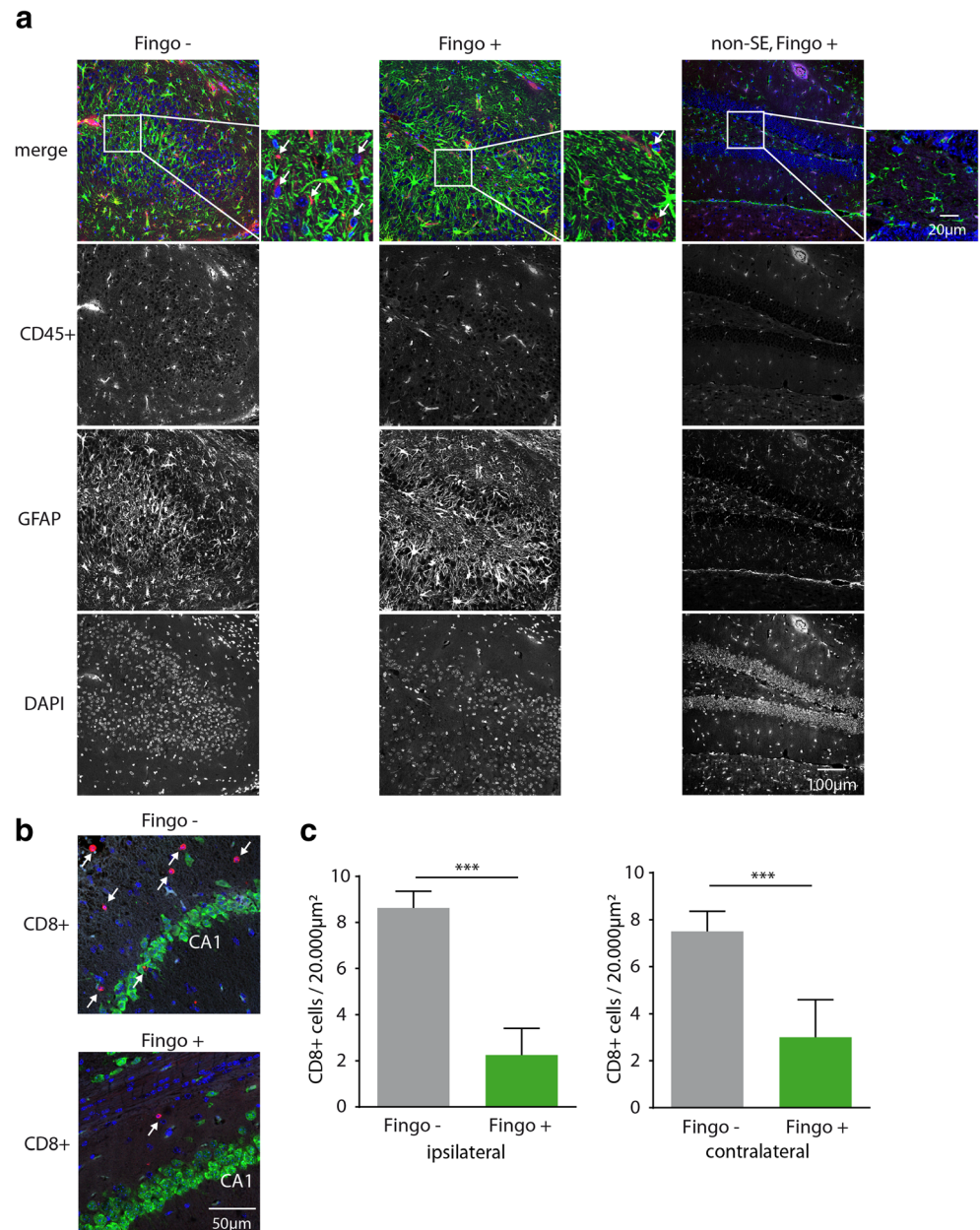
behavioral changes and all animals survived the fingolimod treatment. The ictal and interictal activity attenuating effects after SE were also reflected by the gamma band power (representative gamma power activity of two animals shown in Fig. 6g). Fingolimod-treated mice exhibited a significant reduction of *gamma* band power in the ipsilateral (Fig. 6h) as well as in the contralateral side (Fig. 6i), which was most prominent contralaterally during weeks 3 and 4 after SE. However, early fingolimod treatment did not significantly attenuate neuronal damage, microglia, astroglia, and CD45- or CD8-positive immune cell activation, neither directly after treatment (14 days) nor after 28 days (Suppl. Fig. 4).

Abundant S1PR3 mRNA and Protein Subunits After KA- and Pilocarpine-Induced SE

We further tested mRNA expression patterns of S1PR1 and S1PR3 at different time points after KA- and pilocarpine-induced SE. S1PR1 showed a transiently lower expression in both SE models compared to controls in CA1, which was most prevalent until 72 h after SE (Fig. 7a, c). A strong increase at 10 days after SE was present in CA1 (Fig. 7c). Expression patterns in CA3 and DG were similar to CA1 after pilocarpine-induced SE (Suppl. Fig. 5A, C).

In contrast, we observed a particularly strong but transiently abundant expression augmentation of S1PR3 in both SE

models in CA1 (Fig. 7b, d) with a peak at 36 h after SE on a similar level in all hippocampal subfields (Suppl. Fig. 5C, E) and a peak at 24 h after KA-induced SE in CA1 (Fig. 7b).

Cellular Confinement of S1PR3 Expression Response to Astrocytes After SE

In order to further analyze the expression intensity and localization of S1PR3 on the protein level in epileptic hippocampi, we performed co-immunohistochemistry by using antibodies binding glial fibrillary acidic protein (GFAP) in order to label astrocytes, Iba-1 correspondingly for microglia, NeuN to label neurons and DAPI as a counterstaining at different time points after pilocarpine-induced SE (2, 4, and 7 days). So far, no antibody was available to us to reliably bind and detect S1PR1 protein in paraffin-embedded or fixed free floating tissue why we focused on the expression pattern of S1PR3 in this study. Thereby, we observed a strong abundance of S1PR3 after SE also on the protein level in individual hippocampal regions largely reflecting the corresponding mRNA dynamics with the strongest expression at day 4 after SE in all hippocampal subfields (Fig. 7e). With respect to time-dependent changes of the cellular distribution of S1PR3 in CA1, at 2 days after SE, the expression of S1PR3 was mainly detected in neuronal nuclei and started to be expressed also in astrocytes and neuronal somata (see white arrowheads in Suppl. Fig. 7). Furthermore, at 4 days after SE, a stronger protein signal of S1PR3 was present in astrocytes (see white arrows in Suppl. Fig. 7) and neurons but not in microglia (Suppl. Fig. 6). The cellular expression pattern showed a protein increase in the neuronal somata at day 4 after SE (see the insert in Suppl. Fig. 6 with DAPI co-staining). Interestingly, at 7 days after SE, the expression was still present in the astrocytes and neurons but at lower levels than after 4 days (Suppl. Fig. 7). Overall, a strong increase of GFAP expression was observed in the time period early after SE. Representative control hippocampal tissue without SE showed a very sparse expression of S1PR3 in neuronal nuclei whereas significant astrocytic expression was not detected (Suppl. Fig. 7, upper panels). We observed similar expression patterns of S1PR3 in CA3 (Suppl. Fig. 8) and DG (Suppl. Fig. 9), also with the most abundant levels at 4 days after SE.

Discussion

Knowledge on the potential of fingolimod in epileptic disease conditions had been limited so far. A recent study claimed fingolimod to exert myelin repair as major aspect in mice in a "PTZ kindling" model [25]. Given the generally focal nature of kindling [26], the relevance of the

Fig. 6 Fingolimod has an anti-epileptogenic, disease-modifying effect. **a** Experimental protocol for studying anti-epileptogenic and disease-modifying effects of fingolimod in kainate-induced TLE. Day 0: SE induction and electrode implantation. After 1 h of full-blown SE fingolimod treatment starts for 2 weeks and is discontinued after 2 weeks of high-dose treatment while animals are still under EEG recording. **b** Fingolimod treatment strongly reduces seizure frequency in TLE (untreated: $n = 13$ mice, treated $n = 9$ mice). Two-way ANOVA: Interaction: n.s., $F(1/100) = 2.39$; week: n.s., $F(1/100) = 0.98$; treatment: ****$p < 0.0001$, $F(1/100) = 27.01$; Sidak's post hoc: week 1/2 *$p = 0.012$, week 3/4 ****$p < 0.0001$. **c, d** Representative EEG of spontaneous seizures of an untreated (**c**) and treated (**d**) animal of the contra- and ipsilateral CA1 area. **e** Under fingolimod treatment (week 1/2), seizure duration is significantly reduced comparing treated and untreated animals (two-way ANOVA treatment: $F(1, 309) = 6.772$, **$p = 0.0097$) (untreated: $n = 13$, treated $n = 9$). Whereas stage 5 seizures are significantly shorter in the fingolimod-treated group IV ($p = 0.043$) stage IV seizures are not ($p = 0.28$). **f** Treatment affects also seizure duration when fingolimod treatment was discontinued during week 3/4 (two-way ANOVA: $F(1,401) = 8.597$, *$p = 0.0036$). Seizures stage V are significantly shorter in the treatment group (**$p = 0.0054$) whereas those of stage VI are not different with respect to the duration ($p = 0.4593$)). **g** Representative contralateral *gamma* band activity over the whole analyzed period of 4 weeks of two representative mice. Green vertical lines represent the activity of a treated and black of an untreated animal. Already under high-dose fingolimod treatment (weeks 1 and 2) a lower activity is present, which appears more pronounced after discontinuing the treatment in week 3/4 after SE. Error bars indicate mean ± SEM. **h, i** Quantitative analysis of *gamma* band activity of the ipsilateral (**h**) and contralateral (**i**) EEG recording (untreated: $n = 11$, treated $n = 7$). Treatment strongly affects the *gamma* band activity (two-way ANOVA: ipsilateral **$p = 0.002$, contralateral ***$p = 0.001$) with a significant reduction contralateral in weeks 3 and 4 (contralateral, week 3 *$p = 0.027$, week 4 *$p = 0.015$). Error bars indicate median ± min to max

applied model for focal epilepsy induced by a single transient brain insult remains unresolved. Furthermore, myelin damage does not represent a major pathology aspect of TLE [27]. Our present data suggest several substantial effects of fingolimod in experimental TLE. In this preclinical setting, the mode of action of fingolimod had disease-modifying, chronically anti-convulsive, anti-inflammatory/anti-gliotic and neuroprotective aspects but lacked an ameliorating effect on SE.

Improving therapy options in *chronic* TLE is a major challenge. In a translational perspective, fingolimod target molecules are strongly augmented in expression in human TLE-HS hippocampi, which also maintain substantial astrogliosis and microglia activation, whereas the neurodegeneration is apparently more active at earlier stages of the disease process [28]. The mode of action of fingolimod on a molecular level has been described as binding to S1PRs. As we demonstrate clearly in hippocampal tissue of two SE-induced TLE-models as well as in human biopsy tissue samples of patients with pharmacoresistant TLE, distinct S1P1Rs namely S1P1R1 and S1P1R3 are rather selectively augmented in expression. The multiple modes of action of fingolimod on a cellular level have been suggested, partly
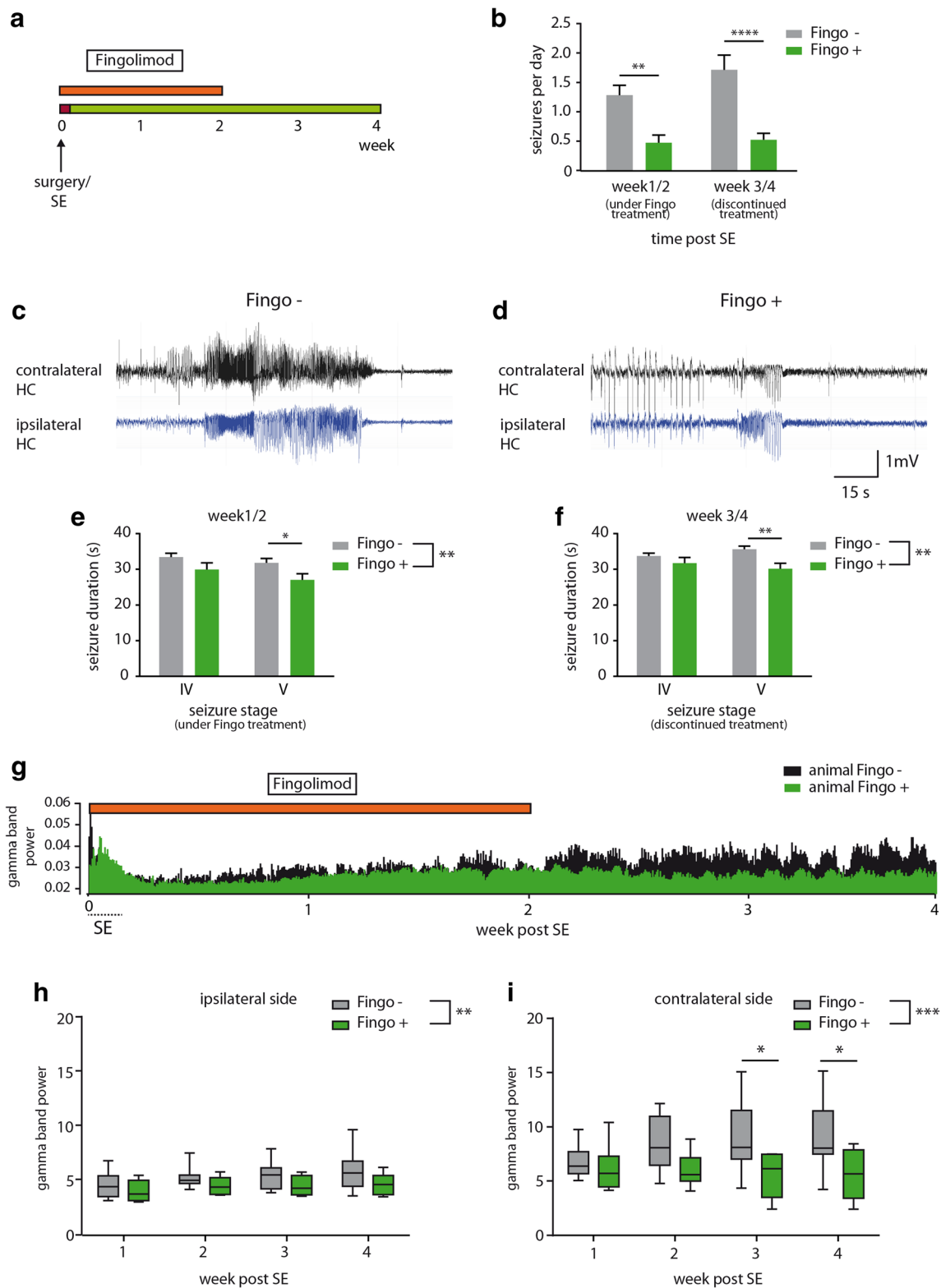
due to the fact that S1P1Rs are expressed by many cell types [29]. The mode of action with respect to cells, which has been mostly focused on due to its role in the context of inflammatory demyelinating disorders of the brain, was

sequestration of lymphocytes in secondary lymphoid organs by downregulation of respective S1P1 receptors [29]. Other modes of action have been suggested as neuroprotective and anti-astrogliotic [30–32]. Our present data clearly
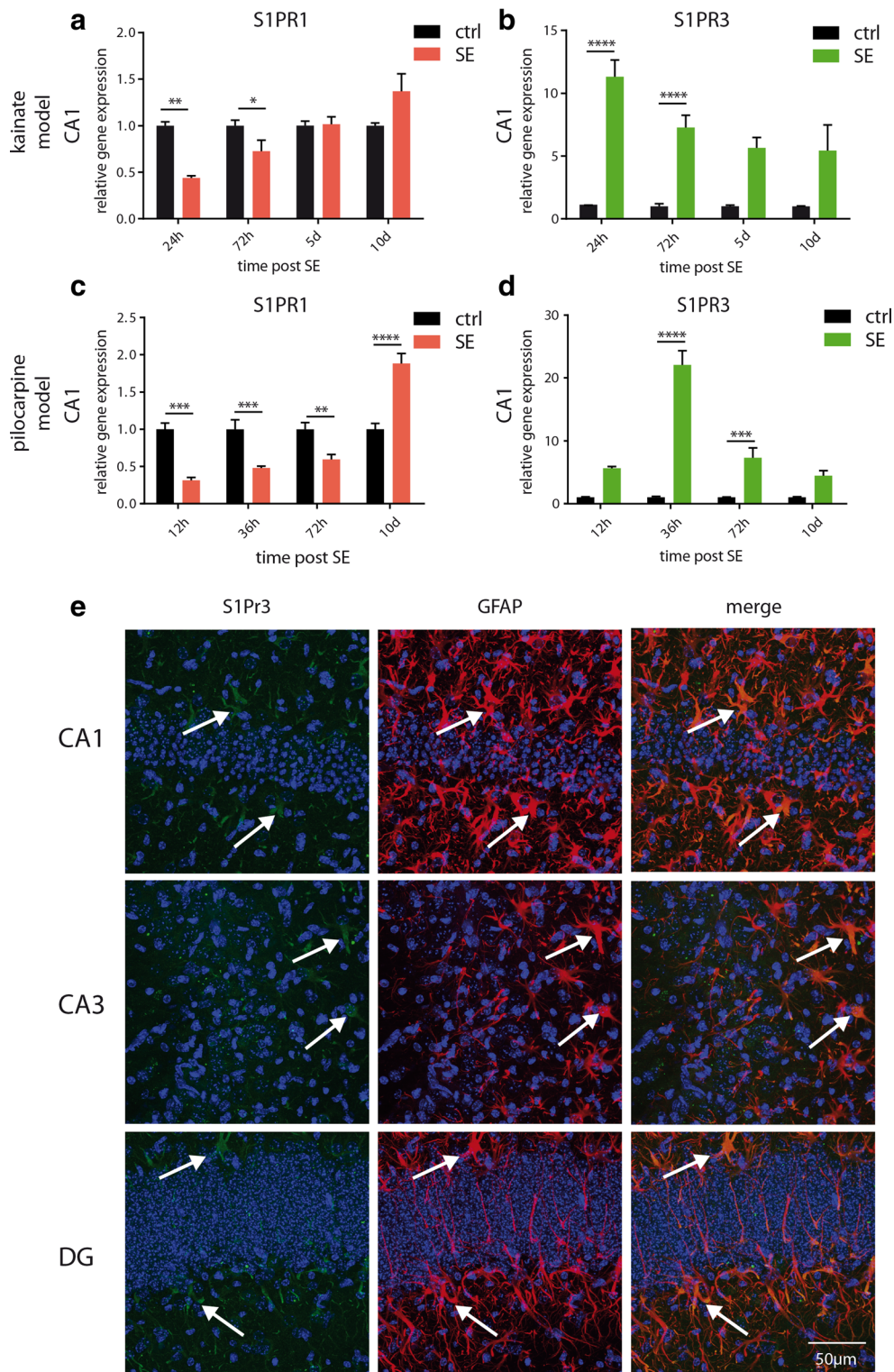
demonstrate that treatment of fingolimod in *chronically* epileptic mice after kainic acid-induced SE ameliorates key features of chronic TLE by reducing seizure activity and attenuation of astrogliosis and the presence of leucocytes.

With respect to a potential anti-epileptogenic effect of fingolimod, data from rats subjected to pilocarpine-induced

SE suggested chronically seizure-attenuating effects [16]. Fingolimod had also anti-epileptogenic effects in a non-SE absence epilepsy model [17]. The respective study demonstrates an anti-epileptogenic effect of fingolimod in a kainic acid-induced post-SE model. However, the drug administration regime may not strongly resemble a realistic clinical

◀ **Fig. 7** Expression analysis of S1PR1 and S1PR3 early after kainate-/pilocarpine-induced SE. **a–d** mRNA expression levels of S1PR1 and S1PR3 after kainate-induced ($n \geq 6$) and pilocarpine-induced ($n \geq 5$) SE in hippocampal CA1. SE strongly affects S1PR1 mRNA levels (two-way ANOVA kainate ****$p < 0.0001$, $F(1,60) = 10.09$; pilocarpine ****$p < 0.0001$, $F(3,33) = 41.61$) as well as S1PR3 (two-way ANOVA kainate ****$p < 0.0001$, $F(1,59) = 136.7$; pilocarpine ****$p < 0.0001$, $F(3,33) = 21.41$). **a** S1PR1 shows a significant reduction of mRNA levels 24 and 72 h after kainate-induced SE (Sidak's post hoc: 24 h **$p = 0.0012$, 72 h *$p = 0.019$). **b** S1PR3 mRNA is strongly increased early after SE (Sidak's post hoc: 24 h ****$p < 0.0001$, 72 h ****$p < 0.0001$). **c** Also after pilocarpine-induced SE, we see an early reduction 12 h (***$p = 0.0007$), 36 h (***$p = 0.0004$), and 72 h (**$p = 0.026$) after SE and an augmentation of mRNA 10 days after (****$p < 0.0001$). **d** In pilocarpine-treated animals, S1PR3 was transiently increased 36 h (****$p < 0.0001$) and 72 h (***$p = 0.0005$) after SE. **e** Representative immunohistochemistry of S1PR3 protein 4 days after SE shows a strong upregulation in co-localization with astrocytes (GFAP, white arrows indicate astrocytic co-localization). Error bars indicate mean ± SEM

scenario, in which most commonly drug administration is started not immediately at the beginning but at more advanced stages of SE. Our present data recapitulates this in a very close fashion. Intriguingly, our data do not show a beneficial effect of fingolimod in the SE phase. In contrast, epileptic EEG characteristics but not the behavioral SE itself were even aggravated under fingolimod treatment in the late SE stage. This aspect is of particular importance. It rules out that the anti-epileptogenic effects of fingolimod that we observe with respect to chronic recurrent seizure activity in respective animals is not due to attenuating effects in the SE stage.

What may be key clinical limitations of fingolimod treatment of patients after potentially epileptogenic brain insults? A severe side effect of fingolimod treatment at the start of administration is given by bradycardia in a subset of patients [33]. This aspect should, however, be manageable by starting fingolimod treatment in an intensive care unit (ICU) as routinely done with MS patients. Our data strongly supports to potential of fingolimod to develop as intriguing disease-modifying, anti-convulsive, and neuroprotective therapy alternative in "pharmacoresistant" TLE patients.

References

1. Loscher W, Klitgaard H, Twyman RE, Schmidt D (2013) New avenues for anti-epileptic drug discovery and development. Nat Rev Drug Discov 12(10):757–776. https://doi.org/10.1038/nrd4126

2. Moshe SL, Perucca E, Ryvlin P, Tomson T (2015) Epilepsy: new advances. Lancet 385(9971):884–898. https://doi.org/10.1016/S0140-6736(14)60456-6

3. Semah F, Picot MC, Adam C, Broglin D, Arzimanoglou A, Bazin B, Cavalcanti D, Baulac M (1998) Is the underlying cause of epilepsy a major prognostic factor for recurrence? Neurology 51(5):1256–1262

4. Johnson AM, Sugo E, Barreto D, Hiew CC, Lawson JA, Connolly AM, Somerville E, Hasic E et al (2016) The severity of gliosis in hippocampal sclerosis correlates with pre-operative seizure burden and outcome after temporal lobectomy. Mol Neurobiol 53(8):5446–5456. https://doi.org/10.1007/s12035-015-9465-y

5. Steinhauser C, Grunnet M, Carmignoto G (2016) Crucial role of astrocytes in temporal lobe epilepsy. Neuroscience 323:157–169. https://doi.org/10.1016/j.neuroscience.2014.12.047

6. Ryan K, Liang LP, Rivard C, Patel M (2014) Temporal and spatial increase of reactive nitrogen species in the kainate model of temporal lobe epilepsy. Neurobiol Dis 64:8–15. https://doi.org/10.1016/j.nbd.2013.12.006

7. Pitkanen A, Engel J Jr (2014) Past and present definitions of epileptogenesis and its biomarkers. Neurotherapeutics 11(2):231–241. https://doi.org/10.1007/s13311-014-0257-2

8. Kaminski RM, Rogawski MA, Klitgaard H (2014) The potential of antiseizure drugs and agents that act on novel molecular targets as antiepileptogenic treatments. Neurotherapeutics 11(2):385–400. https://doi.org/10.1007/s13311-014-0266-1

9. Tsai HC, Han MH (2016) Sphingosine-1-phosphate (S1P) and S1P signaling pathway: therapeutic targets in autoimmunity and inflammation. Drugs 76(11):1067–1079. https://doi.org/10.1007/s40265-016-0603-2

10. Paxinos G, Franklin, K (2012) Paxinos and Franklin's the mouse brain in stereotaxic coordinates, 4th edition.

11. Bedner P, Dupper A, Huttmann K, Muller J, Herde MK, Dublin P, Deshpande T, Schramm J et al (2015) Astrocyte uncoupling as a cause of human temporal lobe epilepsy. Brain 138(Pt 5):1208–1222. https://doi.org/10.1093/brain/awv067

12. Becker AJ, Pitsch J, Sochivko D, Opitz T, Staniek M, Chen CC, Campbell KP, Schoch S et al (2008) Transcriptional upregulation of Cav3.2 mediates epileptogenesis in the pilocarpine model of epilepsy. J Neurosci 28(49):13341–13353. https://doi.org/10.1523/JNEUROSCI.1421-08.2008

13. Pitsch J, Schoch S, Gueler N, Flor PJ, van der Putten H, Becker AJ (2007) Functional role of mGluR1 and mGluR4 in pilocarpine-induced temporal lobe epilepsy. Neurobiol Dis 26(3):623–633

14. Pitsch J, Opitz T, Borm V, Woitecki A, Staniek M, Beck H, Becker AJ, Schoch S (2012) The presynaptic active zone protein RIM1alpha controls epileptogenesis following status epilepticus. J Neurosci 32(36):12384–12395. https://doi.org/10.1523/JNEUROSCI.0223-12.2012

15. Pitsch J, Becker AJ, Schoch S, Muller JA, de Curtis M, Gnatkovsky V (2017) Circadian clustering of spontaneous epileptic seizures emerges after pilocarpine-induced status epilepticus. Epilepsia 58:1159–1171. https://doi.org/10.1111/epi.13795

16. Gao F, Liu Y, Li X, Wang Y, Wei D, Jiang W (2012) Fingolimod (FTY720) inhibits neuroinflammation and attenuates spontaneous convulsions in lithium-pilocarpine induced status epilepticus in rat model. Pharmacol Biochem Behav 103(2):187–196. https://doi.org/10.1016/j.pbb.2012.08.025

17. Leo A, Citraro R, Amodio N, De Sarro C, Gallo Cantafio ME, Constanti A, De Sarro G, Russo E (2017) Fingolimod exerts only temporary antiepileptogenic effects but longer-lasting positive effects on behavior in the WAG/Rij rat absence epilepsy model. Neurotherapeutics 14(4):1134–1147. https://doi.org/10.1007/s13311-017-0550-y

18. Reagan-Shaw S, Nihal M, Ahmad N (2008) Dose translation from animal to human studies revisited. FASEB J 22(3):659–661. https://doi.org/10.1096/fj.07-9574LSF

19. Blümcke I, Pauli E, Clusmann H, Schramm J, Becker A, Elger C, Merschhemke M, Meencke HJ et al (2007) A new clinico-pathological classification system for mesial temporal sclerosis. Acta Neuropathol 113(3):235–244. https://doi.org/10.1007/s00401-006-0187-0

20. Kral T, Clusmann H, Urbach J, Schramm J, Elger CE, Kurthen M, Grunwald T (2002) Preoperative evaluation for epilepsy surgery (Bonn algorithm). Zentralbl Neurochir 63(3):106–110

21. van Loo KM, Schaub C, Pitsch J, Kulbida R, Opitz T, Ekstein D, Dalal A, Urbach H et al (2015) Zinc regulates a key transcriptional pathway for epileptogenesis via metal-regulatory transcription factor 1. Nat Commun 6:8688. https://doi.org/10.1038/ncomms9688

22. Pernhorst K, Herms S, Hoffmann P, Cichon S, Schulz H, Sander T, Schoch S, Becker AJ et al (2013) TLR4, ATF-3 and IL8 inflammation mediator expression correlates with seizure frequency in human epileptic brain tissue. Seizure 22(8):675–678. https://doi.org/10.1016/j.seizure.2013.04.023

23. Jones RT, Barth AM, Ormiston LD, Mody I (2015) Evolution of temporal and spectral dynamics of pathologic high-frequency oscillations (pHFOs) during epileptogenesis. Epilepsia 56(12):1879–1889. https://doi.org/10.1111/epi.13218

24. Kunkel GT, Maceyka M, Milstien S, Spiegel S (2013) Targeting the sphingosine-1-phosphate axis in cancer, inflammation and beyond. Nat Rev Drug Discov 12(9):688–702. https://doi.org/10.1038/nrd4099

25. Gol M, Ghorbanian D, Hassanzadeh S, Javan M, Mirnajafi-Zadeh J, Ghasemi-Kasman M (2017) Fingolimod enhances myelin repair of hippocampus in pentylenetetrazol-induced kindling model. Eur J Pharm Sci 96:72–83. https://doi.org/10.1016/j.ejps.2016.09.016

26. Becker AJ (2017) Animal models of acquired epilepsy: insights into mechanisms of human epileptogenesis. Neuropathol Appl Neurobiol 44:112–129. https://doi.org/10.1111/nan.12451

27. Blumcke I, Cross JH, Spreafico R (2013) The international consensus classification for hippocampal sclerosis: an important step towards accurate prognosis. Lancet Neurol 12(9):844–846. https://doi.org/10.1016/S1474-4422(13)70175-3

28. Aronica E, Crino PB (2011) Inflammation in epilepsy: clinical observations. Epilepsia 52(Suppl 3):26–32. https://doi.org/10.1111/j.1528-1167.2011.03033.x

29. Jeffery DR, Rammohan KW, Hawker K, Fox E (2016) Fingolimod: a review of its mode of action in the context of its efficacy and safety profile in relapsing forms of multiple sclerosis. Expert Rev Neurother 16(1):31–44. https://doi.org/10.1586/14737175.2016.1123094

30. Lee DH, Seubert S, Huhn K, Brecht L, Rotger C, Waschbisch A, Schlachetzki J, Klausmeyer A et al (2017) Fingolimod effects in neuroinflammation: regulation of astroglial glutamate transporters? PLoS One 12(3):e0171552. https://doi.org/10.1371/journal.pone.0171552

31. Rothhammer V, Kenison JE, Tjon E, Takenaka MC, de Lima KA, Borucki DM, Chao CC, Wilz A et al (2017) Sphingosine 1-phosphate receptor modulation suppresses pathogenic astrocyte activation and chronic progressive CNS inflammation. Proc Natl Acad Sci U S A 114(8):2012–2017. https://doi.org/10.1073/pnas.1615413114

32. Das A, Arifuzzaman S, Kim SH, Lee YS, Jung KH, Chai YG (2017) FTY720 (fingolimod) regulates key target genes essential for inflammation in microglial cells as defined by high-resolution mRNA sequencing. Neuropharmacology 119:1–14. https://doi.org/10.1016/j.neuropharm.2017.03.034

33. Calabresi PA, Radue EW, Goodin D, Jeffery D, Rammohan KW, Reder AT, Vollmer T, Agius MA et al (2014) Safety and efficacy of fingolimod in patients with relapsing-remitting multiple sclerosis (FREEDOMS II): a double-blind, randomised, placebo-controlled, phase 3 trial. Lancet Neurol 13(6):545–556. https://doi.org/10.1016/S1474-4422(14)70049-3